Supplementary Information: A Novel Microfluidic Approach to Quantify Pore-Scale Mineral Dissolution in Porous Media

Rafid Musabbir Rahman[1], Elliott Niemur[1], Gianluca Blois[2], Farzan Kazemifar[3], Myeongsub Kim[4], and Yaofa Li[1,5,*]

[1]Montana State University, Department of Mechanical & Industrial Engineering, Bozeman, MT 59717, USA.
[2]University of Idaho, Department of Mechanical Engineering, Boise, ID 83702, USA.
[3]San Jose State University, Department of Mechanical Engineering, San Jose, CA 95192, USA.
[4]Florida Atlantic University, Department of Ocean and Mechanical Engineering, Boca Raton, FL 33431, USA.
[5]University of California, Riverside, Department of Mechanical Engineering, Riverside, CA 92521, USA.
[*]yaofa.li@ucr.edu

ABSTRACT

Mineral dissolution in porous media coupled with single- and/or multi-phase flows is pervasive in natural and engineering systems. Dissolution modifies the physical, hydrological, and geochemical properties of the solid matrix, resulting in a complex coupling between local dissolution rate and pore-scale flow. The work reports an innovative microfluidic approach that includes novel 2D reactive porous media and advanced pore flow diagnostics for the study of pore-scale dissolution in porous media with unprecedented details. The 2D microfluidic porous media, called micromodels, were fabricated in calcite by combining photolithography and wet etching, which not only offers precise control over the structural and chemical properties, but also facilitate unobstructed optical access to the pore flow, significantly improving over existing methods. We believe the work represents the first of its kind as it for the first time directly applies photolithography to calcite samples and demonstrates the use of particle image velocimetry to investigate chemical reactions in porous media. The preliminary results have revealed the crucial roles of local concentration gradients in mineral dissolution and call for reconsideration of many assumptions used in the current modeling tools, which paves the way for renewed fundamental understanding of reactive transport and improved modeling tools with better accuracy.

Experimental Procedure

Apparatus and working fluid

To perform flow measurements with the calcite-based micromodel, an experimental apparatus was constructed around an inverted epi-fluorescence microscope (Olympus, IX71) as shown in Fig. S1. The micromodel was mounted on an automated translation stage, with the inlet and outlet connected to a syringe pump (Harvard Apparatus, PHD2000) and a glass beaker serving as a waster container, respectively. The microscope was equipped with a green LED (Thorlabs, SOLIS-525C) and a scientific CMOS camera (Andor, Neo 5.5 sCMOS), which are in turn synchronized and controlled by a function generator (Berkeley Nucleonics, 565-4C) and a PC. The LED and the camera were used to illuminate and image the flow, respectively.

As a proof-of-concept and a demonstration of the micromodel capability, the preliminary tests presented in this study used 0.01% HCl (or water for micro-PIV test) as the working fluid to ensure a controlled reaction with the calcite. This combination was chosen for its simple dissolution kinetics as dictated by[1],

$$\mathrm{CaCO_3(s) + 2HCl(aq) \rightarrow CaCl_2(aq) + CO_2(aq) + H_2O(l)} \tag{1}$$

As detailed below, to perform fluorescent microscopy, the working fluid was tagged with a fluorescence dye, Rhodamine B (RhB, Acros Organics, 98+% pure, CAS:81-88-9), whereas for the micro-PIV measurements, the working fluid was seeded with 1-μm polystyrene fluorescent particles (Invitrogen F8819). For the fluorescent microscopy, a 0.5% HCl stock solution was prepared by diluting a 37% HCl solution with DI water, whereas a 10 mM RhB stock solution was prepared by dissolving 47.9 mg RhB powder in 100 ml DI water. Then 0.5 ml RhB stock solution, 0.16 ml 0.5% HCl solution, and 7.34 ml DI water were mixed, resulting in the final HCl and RhB concentrations of 0.01% and 0.625 mM, respectively. Similarly, for the micro-PIV, 10 μl stock solution containing particles of 1 μm in diameter (2% v/v solid), 0.165 ml of 0.5% HCl stock solution, and 7.835 ml of DI water were mixed, resulting in the final HCl concentration of 0.01%, and a particle volume fraction of

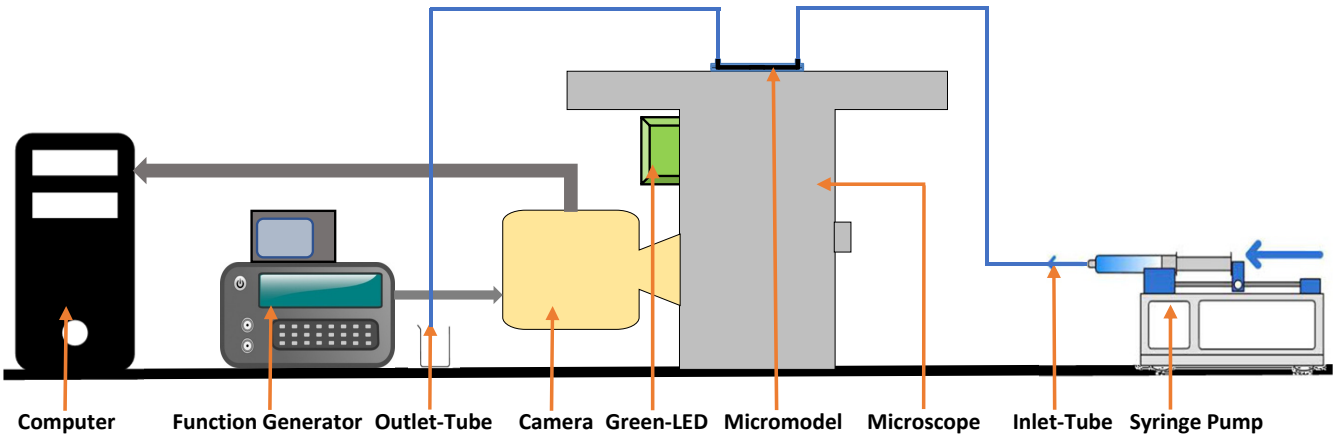

Figure S1. Schematic diagram of the experimental setup. The apparatus is constructed around an inverted epi-fluorescence microscope (Olympus, IX71), which is equipped with a green LED (Thorlabs SOLIS-525C) and a CMOS camera (Andor, Neo 5.5 sCMOS). The camera and LED are both controlled and synchronized by a function generator and a PC. The micromodel is mounted on the translation stage of the microscope, the flow through which is controlled by a syringe pump (Harvard Apparatus, PHD 2000).

2.5×10^{-5}. The polystyrene particles have a density of 1.05 g/ml, which closely matches that of water, ensuring that the particles are "neutrally buoyant" and thus faithfully follow the flow. The volume fraction of solid particles was kept low to avoid significant alterations in the properties of the aqueous phase. A new micromodel was used for each experimental run, and the flow rates were kept at 50 μl/min and 0.02μl/min, corresponding to nominal Reynolds numbers of 7.5 and 3×10^{-3} based on the average pore diameter, for the fluorescent microscopy and micro-PIV experiments, respectively.

Fluorescent microscopy

In the fluorescent microscopy measurement, the LED light source (Thorlabs SOLIS-525C) with a nominal wavelength of 525 nm filtered by a bandpass filter (HQ 535/50) was used to illuminate the sample. The emitted fluorescence from the flow was passed through another bandpass filter (HQ 610/75), focused by a 4x microscope objective (Olympus PLN 4x) to the camera (Andor Neo 5.5). As shown in Fig. S2a, the field of view (FOV) created with this configuration is $4.16\times1.95\,\mathrm{mm}^2$, and the solid grain and aqueous phase appear as the dark and bright regions, respectively. Grayscale images were captured at 2 frames per second (fps), which was sufficient to temporally resolve the dynamic evolution of the geometry of the solid matrix[2]. The acquired gray-scale images were then analyzed and segmented using an in-house MATLAB code based on the intensity of each pixel[3]. The instantaneous spatial distribution and area of the grains were calculated by counting the number of pixels occupied by the white regions as shown in Fig. S2b. Additionally, once the solid and liquid phases were identified, the interfaces were determined by finding the edges of the solid phase, further producing quantification of the interfacial area for reaction. It is worth noting that this single-color microscopy is only able to differentiate the aqueous phase which is tagged with the fluorescent dye (bright regions herein), whereas all other phases including the solid grains and any gaseous phase, potentially trapped and/or produced by the reaction, all appear as dark regions as shown in Fig. S2a. However, in this particular experiment, the gas phase shows up slightly brighter than the background grains, presumably due to the presence of the gas-liquid interfaces that help scatter fluorescent light, allowing us to manually separate the gas phase from the grains. This manual processing step was possible due to the fact that the trapped gas bubbles do not substantially change over time, making this task feasible with a reasonable amount of manual effort. Although the present optical setup was sufficient to perform the current experiments, where reaction-produced CO_2 was instantaneously dissolved in the aqueous phase, more rigorous quantification of a three-phase flow with the CO_2 evolving as a separate phase will necessitate the use of dual-color fluorescent microscopy as demonstrated in our previous work[4,5].

Particle image velocimetry

In micro-PIV, the experimental setup and procedures are largely similar to that used in the fluorescence microscopy with three major modifications: 1) instead of fluorescent dye, the aqueous phase was seeded with 1 μm neutrally buoyant fluorescent particles as flow tracers (ThermoFishere F8823); 2) a 10x objective was used for better spatial resolution, producing a smaller FOV ($1.66\times1.40\,\mathrm{mm}^2$); 3) the camera was run at a higher frame rate (20 fps) to temporally resolve the flow. Two consecutive images of the particles are recorded with a prescribed time delay, $\Delta t = 50$ ms. The LED was pulsed by the function generator to produce an effective exposure time of 5 ms per frame, which is critical to avoid any streaks of the tracer particles as they

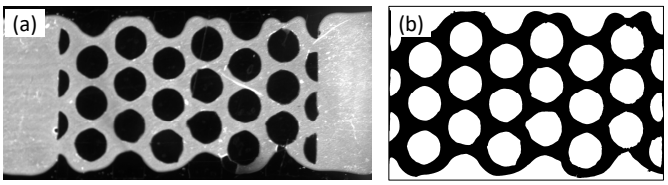

Figure S2. (a) A raw gray-scale fluorescent image with the aqueous phase and the grains shown as bright and dark regions, respectively; (b) a segmented image with the aqueous phase and the grains shown as black and white regions, respectively. The segmented image was cropped to show the region of interest only (ROI). We note that in this particular micromodel only four rows of micropillars were formed in the porous section, as opposed to the five rows in the original design. This was caused by slightly excessive etching in step IV, leading to a microchannel that is slightly narrower than the designed width of 2 mm. This issue can be mitigated and eliminated by making the designed channel width slightly greater than the porous section width.

travel with the flow. To generate velocity vector fields from the raw images of particles, image masking was first applied to each image to identify the locations of the solid grains and trapped gas bubbles, where tracer particles were not present. Then each image was subdivided into small areas, called interrogation windows. The average displacement of the tracer particles $\Delta\mathbf{x}$ within each interrogation window was determined statistically from cross-correlation analysis of consecutive images. The velocity vector $\mathbf{u}$ for each interrogation window was then obtained by dividing the displacement $\Delta\mathbf{x}$ by the prescribed Δt[6]. In this study, 1000 raw micro-PIV images were processed with a multi-pass approach combined with the correlation averaging scheme[7] employing the open source MATLAB code, PIVlab[8]. The size of the interrogation windows was 64×64 pixels, with 50% overlap, which yielded a spatial resolution of 84 μm and a velocity vector spacing of 42 μm.

References

1. Song, W., de Haas, T. W., Fadaei, H. & Sinton, D. Chip-off-the-old-rock: the study of reservoir-relevant geological processes with real-rock micromodels. *Lab on a Chip* **14**, 4382–4390 (2014).
2. Singh, R. *et al.* Real rock-microfluidic flow cell: A test bed for real-time in situ analysis of flow, transport, and reaction in a subsurface reactive transport environment. *J. contaminant hydrology* **204**, 28–39 (2017).
3. Li, Y., Blois, G., Kazemifar, F. & Christensen, K. T. High-speed quantification of pore-scale multiphase flow of water and supercritical co2 in 2-d heterogeneous porous micromodels: Flow regimes and interface dynamics. *Water Resour. Res.* **55**, 3758–3779 (2019).
4. Blois, G., Barros, J. M. & Christensen, K. T. A microscopic particle image velocimetry method for studying the dynamics of immiscible liquid–liquid interactions in a porous micromodel. *Microfluid. Nanofluidics* **18**, 1391–1406 (2015).
5. Kazemifar, F., Blois, G., Kyritsis, D. C. & Christensen, K. T. A methodology for velocity field measurement in multiphase high-pressure flow of co2 and water in micromodels. *Water Resour. Res.* **51**, 3017–3029 (2015).
6. Santiago, J. G., Wereley, S. T., Meinhart, C. D., Beebe, D. J. & Adrian, R. J. A Particle Image Velocimetry System for Microfluidics. *Exp. Fluids* **25**, 316–319, DOI: 10.1007/s003480050235 (1998).
7. Meinhart, C. D., Wereley, S. T. & Santiago, J. G. A piv algorithm for estimating time-averaged velocity fields. *J. Fluids Eng.* **122**, 285–289 (2000).
8. Thielicke, W. & Sonntag, R. Particle image velocimetry for matlab: Accuracy and enhanced algorithms in pivlab. *J. Open Res. Softw.* **9** (2021).